Viscous damping of microcantilevers with modified surfaces and geometries

Ergincan, O.; Palasantzas, G.; Kooi, B. J.

Published in:
Applied Physics Letters

DOI:
10.1063/1.4744951

Publication date:
2012

Viscous damping of microcantilevers with modified surfaces and geometries

O. Ergincan, G. Palasantzas,[a] and B. J. Kooi
Zernike Institute for Advanced Materials, University of Groningen, 9747 AG Groningen, The Netherlands

(Received 11 July 2012; accepted 25 July 2012; published online 7 August 2012)

Noise measurements were performed to determine the quality factor Q and the resonating frequency shift as a function of gas pressure P for microcantilevers with modified surfaces and geometries. In the molecular and continuum regimes, energy loss is dominated by the surrounding fluid leading to reduction of the Q factor and shift of the resonance frequency by Δf, which becomes significant in the continuum regime showing sensitivity on surface changes. This is shown via three methods: frequency shift Δf vs. P, Q factor vs. P, and direct calculation using surface roughness details acquired via atomic force microscopy. © *2012 American Institute of Physics*. [http://dx.doi.org/10.1063/1.4744951]

A relentless effort is underway in microelectronics technology to push deep into the submicron range by extending microelectromechanical systems (MEMS) to the nanometer range, i.e., towards nanoelectromechanical systems (NEMS).[1–9] As a result we can obtain extremely high fundamental frequencies in the microwave range,[4,10] while preserving very high mechanical responsivity with mechanical quality factors $Q \sim 10^3$–10^5,[4,11] active masses of femtograms ($\sim 10^{-15}$ g),[4] ultra-low heat capacities ($<10^{-18}$ cal),[12] etc. This combination of properties translates, for example, to high force and mass sensitivity.[13] A central topic of fundamental and applied research in MEMS/NEMS is the achievement of high Q factors. The latter measures the ratio of the stored energy E_{stor} to the dissipated energy E_{dis} within an oscillation cycle, and it is defined by the relation $Q = 2\pi(E_{stor}/E_{dis})$. The higher the Q factor the higher is the sensitivity of the resonance system to external perturbations. The Q factor determines also the level of fluctuations that degrades the spectral purity of a resonance (linewidth broadening), and the minimum intrinsic power at which the device must operate ($\sim k_B T/Q$).[4] The Q factor of a resonator is determined by various loss mechanisms and it can be approximated by the relation $Q^{-1} = \sum_j Q^{-1}$. The index j includes, for example, attachment loss from gas molecules impinging the resonator, losses due to bulk and surface defects and impurities, thermoelastic losses (thermal currents generated by vibratory volume changes in elastic media with nonzero thermal-expansion coefficient), and losses due to phonon scattering (interaction between oscillatory sound waves and thermal phonons).[14]

Up to now, a variety of studies have shown that surface roughness influences the quality factor for operation in vacuum.[15–18] The quality factor of Si nanowires, with 45 nm beam widths and 380 MHz resonating frequencies, was decreased from ~3000 to 500 by an increment of the surface area to volume ratio from ~0.02 to 0.07.[15] Studies for SiC/Si resonators have shown that devices operational in the UHF/microwave regime had a low surface roughness (~2.1 nm), while devices with rougher films (up to ~7.1 nm) were operational up to the VHF range.[16] Recent studies have shown theoretically that random surface roughness affects the quality factor, limit to mass sensitivity, Allan variance, and dynamic range of resonators.[17,18] Moreover, noise measurements were performed to determine the quality factor (Q) as a function of gas pressure P as in Ref. 19 but for cantilevers with systematically modified surfaces.[20] At higher pressures, within the molecular regime, Q showed the typical inverse linear dependence on pressure $Q \sim P^{-1}$.[19] However, in the molecular regime the Q factor also showed a strong dependence on surface morphology as indicated by surface areas calculations using measured roughness data obtained by atomic force microscopy (AFM), and compared to those obtained from $Q \sim P^{-1}$ plots.[20]

However, so far a detailed systematic experimental study of the influence of surface area on the Q factor of resonators within the continuum regime, where dissipation is the highest, is still missing. Hence, this will be the topic of the present paper, where we explore the dependence of the Q factor on the surface area of commercial microcantilevers (Fig. 1) at various gas pressures, covering for completeness the whole range, from the free molecular up-to the continuous regime (reaching ambient pressures ~1 atm). To modify the effective surface areas of the cantilevers in contact with the fluid (gas or liquid), we used two well-known techniques; the focused ion beam (FIB) etching technique and co-sputtering of a metal film. FIB was also used for altering the geometry of some of the resonators. The purpose of varying the techniques and types of sample geometry is to broaden the perspective to understand in a wide pressure range the effect of surface areas on the Q factor of the resonators.

Commercially available microcantilevers are used for surface modification due to the ease of handling them and relative purity in their manufacturing process (Table I). Scanning electron microscopy (SEM) was used to acquire the cantilever dimensions (Table I). Notably, even for the samples of the same batch dimensions may vary ~10% for each axis. Samples (S) that were not modified are denoted as S1 and S2 and they have different dimensions and cross-section geometry. Samples S3 and S4 have been etched using FIB forming grooves ≈200 nm apart from each other (Figs. 1(a) and 1(b)) either parallel to the wave propagation along

[a]Author to whom correspondence should be addressed. Electronic mail: G.Palasantzas@rug.nl.

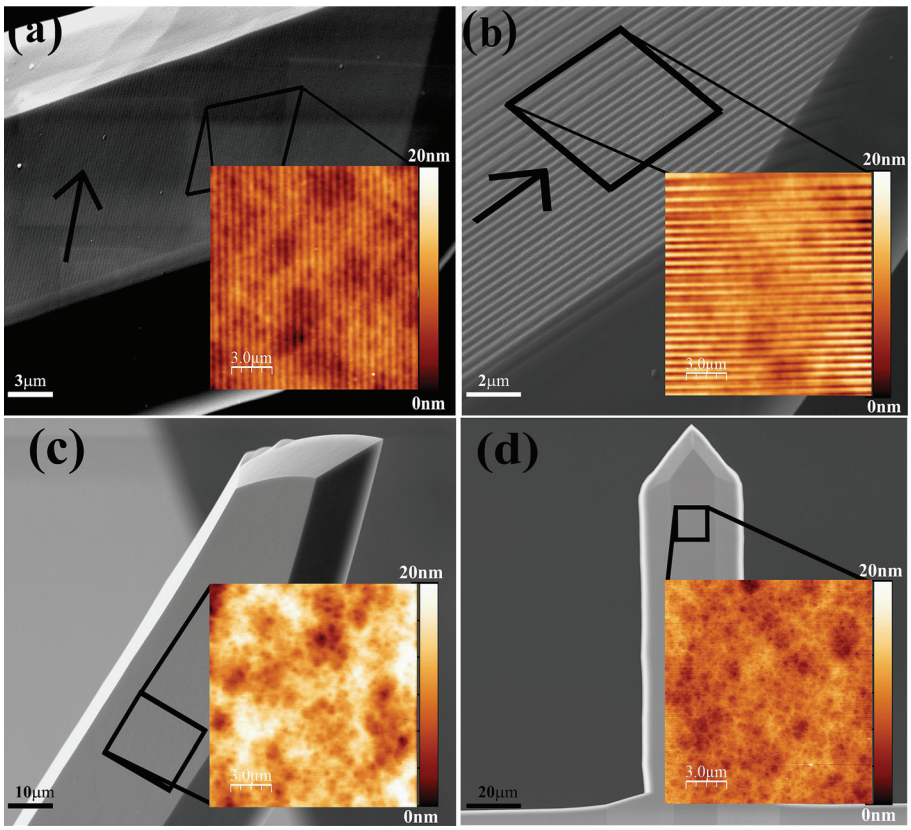

FIG. 1. SEM images and the corresponding AFM topography images of the samples with the same height scale: (a) S4 sample: FIB modifed surface and grooves are parallel to the width of the resonator, (b) S5 sample: FIB modifed surface and the grooves are parallel to the lenght of the resonator, (c) S3 sample: coated with Ge_7Sb_{93}, (d) S1 sample: nonmodified resonator.

the length of the resonator S3 or normal to the wave propagation (along the width) of the resonator S4. The sample S5 was co-sputtered with 50 nm thick Ge_7Sb_{93} thin films. Finally, the samples S6 and S7 have been geometrically modified in the clamping area of the cantilever to its support block by removing mass (Figs. 2(b) and 2(c)).

The noise measurements for the determination of the Q factor were performed at room temperature using the thermal tuning (Q-tuning) method[3] and placing the AFM head into a vacuum bell-jar system with controlled pressure from ambient down to $\sim 10^{-6}$ mbar. The Q-tuning method, which was developed for the determination of cantilever spring constants (k) with accuracy down to $\sim 5\%$,[3] involves measuring the cantilever's mechanical response due to agitations of impinging molecules from the surrounding fluid (ambient air, gases, and liquids) and due to thermal dissipation via internal degrees of freedom.[3] The AFM hardware measures the cantilever's fluctuations as a function of time from which, by Fourier transformation, the frequency dependent power spectral density (PSD) $|A(\omega)|$ is obtained. Fitting the PSD spectrum $|A(\omega)|$ with a Lorentzian form $|A(\omega)|^2 = A_o/[(\omega^2 - \omega_o{}^2)^2 + (\omega\omega_o/Q)^2]$ (Ref. 3) where ω_0 the radial resonance frequency of the free cantilever, and after data averaging of multiple PSD spectra, the averaged Q factor (both due to intrinsic and fluidic or gas dissipation) is obtained. The noise measurements were repeated more than eleven times at each pressure to avoid the influence of instantaneous measurement errors such as jitter effect, etc. and to confirm repeatability of the measurement. The acquired data were averaged allowing one to obtain the quality factor Q with an accuracy of $\sim 10\%$. Notably, extensive analysis of cantilever heating effects in both air and vacuum resulted in negligible frequency shifts $\Delta\omega_0 \sim 10$–20 Hz ($\sim 10^{-3}\%\ \omega_o$). Finally, the high pressure range measurement of the PSD

TABLE I. List of investigated samples and summary of results. $S_{Total,1}$, total effective surface area from the fittings in Fig. 2; $S_{Total,2}$, total effective surface area from the fittings in Fig. 3; $S_{Total,3}$, total effective surface area calculated by ρ_{rms} (S1, S6, S7 $\sim$ 0.0018, S2 $\sim$ 0.0046, S3 $\sim$ 0.0016, S4 $\sim$ 0.007, S5 $\sim$ 0.006) as obtained from AFM line profiles.

	Dimensions[a] (μm)	Frequency (kHz)	Type[b]	$S_{Total,1} \times 10^{-9}$ (m^2)	$S_{Total,2} \times 10^{-9}$ (m^2)	$S_{Total,3} \times 10^{-9}$ (m^2)	$S_{Total,1/3}$	$S_{Total,1/2}$
S1	$15 \times 35 \times 130 \times 4$	342.7	a	2.13	1.29	2.13	1.00	1.65
S2	$90 \times 500 \times 0.99$	38.3	d	15.6	9.15	19.9	0.78	1.70
S3	$25 \times 47 \times 141 \times 4.1$	311.2	a	2.35	1.55	2.68	0.88	1.52
S4	$18 \times 38 \times 131 \times 3.9$	340.3	a	1.80	1.26	1.97	0.91	1.43
S5	$15 \times 35 \times 131 \times 4.1$	312.6	a	2.12	1.14	2.18	0.97	1.86
S6	$18 \times 35 \times 88 \times 3.95$	181.3	b	1.36	0.89	1.27	1.07	1.53
S7	$18 \times 35 \times 112 \times 3.9$	227.4	c	1.55	0.90	1.59	0.97	1.72

[a]For the trapezoidal shape beam, the dimensions are: (width_top $\times$ width_bottom $\times$ length $\times$ thickness), and for rectangular beam (type d) the dimensions are: (width $\times$ length $\times$ thickness).
[b]Type notation is the same as used for the inset of Fig. 2.

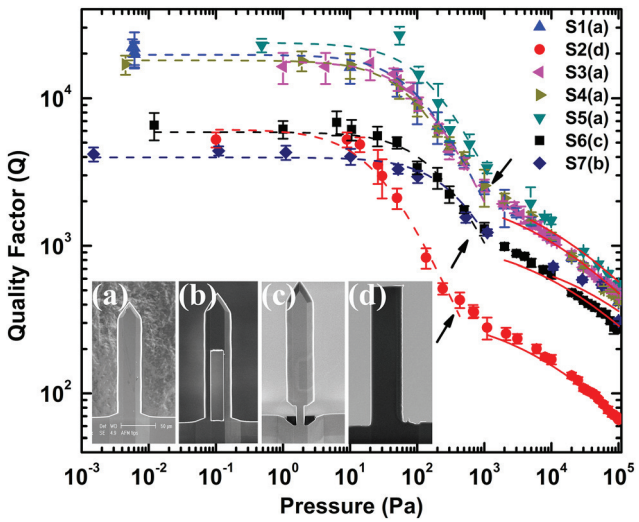

FIG. 2. Quality factor (Q) vs. P. The samples S1 (trapezoid, Fig. 1(d)) and S2 (rectangular) are shown as insets. (a) and (b) are non-modified surface cantilevers. Samples S3 (Fig. 1(a)) and S4 (Fig. 1(b)) are modified cantilevers on the top surfaces but in different etching directions as shown in Fig. 1. S5 is FIB modified inset (b), and S6 is FIB modified inset (c). The fits by the solid lines illustrate the $\sim 1/P$ scaling in the molecular regime,[20] and that of Eq. (2) for the continuum regime. The arrows show the transition point from the molecular to the dense regime ($\omega\tau \approx 1, = 1850/P$ (Ref. 19)).

spectra increases the necessity of an accurate pressure measurement. Because the accuracy of a full range pressure gauge drops at high pressures, it is necessary to use a gas independent, diaphragm pressure gauge, for a more accurate pressure measurement. It was experienced up to 80% difference between the full range pressure gauge (Varian FRG-700), and the high pressure, gas independent, diaphragm gauge (Vacuubrand DVR-2).

Furthermore, in the measurement plots of the Q factor and frequency shift (Δf) vs. P there are four regimes of interest (Figs. 2 and 3). The first one is the intrinsic regime, the so-called free molecular regime, where the number of molecules impinging (molecule mean free paths ≪ resonator size) the resonator is low enough so that it can be neglected and energy losses are dominated by intrinsic resonator mechanisms. In this regime, Q factor and frequency are constant and independent of pressure P. The second regime is called the molecular regime where the oscillation is damped due to momentum exchange with a dilute gas of noninteracting molecules, where the Q factor scales down with pressure as $Q \sim P^{-1}$.[19] The effect of local roughness and surface area in this regime has been recently explored and good agreement was found between results obtained from $Q \sim P^{-1}$ plots and direct surface area calculations from AFM analysis.[20] The third regime is the transition where a crossover from the non-Newtonian molecular regime to continuum or dense flow regime occurs. The Newtonian approximation, the basis for the Navier-Stokes equations, breaks down when the particulate nature of the fluid becomes significant to the flow. In this case, it is common to consider the validity of the Newtonian approximation by comparing the mean free path λ in the medium to an ill-defined characteristic length (e.g., the width of the cantilever w). In the fourth regime or continuum regime, a transition from Newtonian ($\omega\tau \ll 1$) to non-Newtonian ($\omega\tau \gg 1$) flow occurs at $\omega\tau \approx 1$ with τ a fluid relaxation time ($\sim 1/P$).[19]

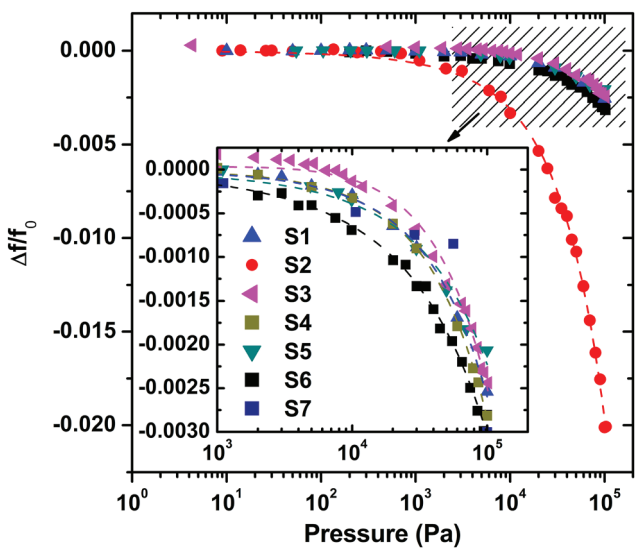

FIG. 3. Normalized frequency change $\Delta f/f_o$ vs. P. The linear part changes at $\omega\tau \approx 1$ for pressures approximately at 10^2 Pa. The inset shows the magnified continuum regime for samples with smaller surface areas as shown for the indicated window. Types of the resonators are indicated with letters similar to Fig. 2 inset. All the fittings were performed via Eq. (2). Notations of the samples are the same as in Fig. 2.

For our cantilevers in the pressure ranges between $\sim 10^2$ Pa and 10^5 Pa, the gas acts as a viscous fluid and the ambient damping can be calculated using fluid mechanics.[19] In this case, the relative frequency shift is given by[21,22]

$$\frac{\Delta f}{f_0} = \frac{\Delta\omega}{\omega_0} = -\frac{\pi b S_{Total,1}}{24 M_{eff}} \frac{M}{RT} p - \frac{3\pi S_{Total,1}}{8 M_{eff}} \sqrt{2\mu \frac{M}{RT}} \sqrt{\frac{p}{\omega_0}}. \quad (1)$$

In Eq. (1), m_b is the mass of the resonator, R the gas constant, T the absolute temperature, M the molar mass of the gas, p the pressure, μ the dynamic viscosity of the gas, ω_0 the resonance frequency in vacuum, and $\Delta\omega$ the shift in resonance frequency. One of the crucial parameters for the calculation of the effective surface area is the effective mass, M_{eff}. The values for M_{eff} have been obtained using both geometric means and experimentally determined cantilever spring constant (k_{eff}) via the resonance frequency $\omega_0 = (k_{eff}/M_{eff})^{1/2}$.[20] Indeed, one obtains the experimental cantilever spring constant k_{eff} by the Q-tuning method.[3] Hence from the first resonance frequency of the cantilever, one obtains a $M_{eff} \approx 23.5\%$ M_T with M_T the total mass of the cantilever.[20] In addition, the Q factor is given by[21,22]

$$Q_{Fluid} = \frac{2 M_{eff} w^2 \omega_0}{S_{Total,2}\left(6\pi\mu w + (3\pi w^2/2)\sqrt{2\mu(M/RT)\omega_0 p}\right)}. \quad (2)$$

Both Eqs. (1) and (2) yield the total effective surface area S_{total} of the cantilever denoted with different index for Q and Δf. Finally, for consistency an analytical estimation of S_{total} was also performed using AFM data. For the rough area calculations, we used the expression[23]

$$S_{rough} \;/\; S_{smooth} \approx \int_0^{+\infty} du \sqrt{1 + \rho_{rms}^2 u} e^{-u} \quad (3)$$

with ρ_{rms} the average local surface slope.[23,24] In all cases, ρ_{rms} was estimated from AFM profile analysis of cantilever surfaces (Fig. 1, insets). Therefore, we can define the effective total surface area of the cantilever as $S_{Total,3} = \sum S_{rough} + \sum S_{smooth}$. For the resonators with the trapezoidal cross section area, the inclined side wall area is also taken into account for the calculation of $S_{Total,3}$.

In order to show the effect of the surface area on the Q factor and the frequency shift Δf, measurements were performed for different types of microcantilevers with varying frequencies, dimensions, and surface modifications. We have investigating the viscous regime because any measurable frequency changes occur for pressures above 10^2 Pa and after the transition regime. In the continuum regime, where the dominant loss mechanism is due to the viscous damping by the fluid, the total effective surface area also plays an important role together with the resonance frequency. The point of the transition from the molecular (fits are also indicated for $Q \sim 1/P$) to continuum regime is indicated in Fig. 2 by an arrow for each individual resonator ($\omega\tau \approx 1$). In the continuum regime, the mass loading of the fluid has several effects: The first one is the frequency shift due to mass loading, and the second one is the change in the characteristic properties such as the cantilever spring constant due to the new effective mass of the system. The large differences in the sizes of the resonators studied here require the validation of Eqs. (1) and (2) and also comparison to analytical calculations.

The total surface area, denoted as $S_{Total,1}$, is obtained by fitting Eq. (1) for the relative frequency shift $\Delta f/f_o$ vs. P data in Fig. 3. The total surface area, denoted as $S_{Total,2}$, is obtained by fitting Eq.(2) for the Q factor vs. P data in Fig. 2. Alternatively, the total effective surface area, denoted as $S_{Total,3}$, is also calculated using the average local slope ρ_{rms} from AFM topography images as in Fig. 1. The results in Table I show that analytical calculations $S_{Total,3}$ and $S_{Total,1}$ agree very well apart from the sample with a very large geometrical surface area (S2). On the other hand, the $S_{Total,2}$ obtained from the Q factor measurements needs a correction factor of approximately 1.62 (averaged value of the area ratios $S_{Total,1/2}$ in Table I). The contribution of the losses in the intrinsic regime via the intrinsic quality factor Q_{int} cannot bridge the deviation in the calculation of $S_{Total,2}$. The deviations between the obtained $S_{Total,2}$ and the other two measurement types ($S_{Total,1}$, and $S_{Total,3}$ (Ref. 20)) in the viscous regime are attributed partly to be result of the change in the mechanical properties of the resonators due to mass loading, which it is not taken into account for the Q factor calculations and it has to be further addressed. This also indicates the importance of surface area calculations for a better understanding of the change in the mechanical properties of the resonators due to mass loading. However, for evaluating the frequency shift Δf in the viscous regime due to mass loading the increase in surface area due to surface roughness is shown to be a crucial parameter.

In conclusion, the dissipation caused by the effective surface area in contact with the surrounding fluid was experimentally measured and analytically calculated by correcting the increase in the effective surface area caused by existing or deliberately introduced surface roughness. It was shown that the effective surface area determination using the normalized frequency shift is more accurate in the continuum regime. However, the Q factor appears to be more sensitive to surface area changes in the molecular regime,[20] while this is not happening in the continuum regime. In any case, these studies show the important effect the effective surface area has on resonating properties, and it has to be taken carefully into account in resonator designs for improved sensing properties.

The authors would like to acknowledge financial support by the STW Grant 10082, useful discussions with V. B. Svetovoy, and G. H. ten Brink for the SEM images.

[1]A. B. Hutchinson, P. A. Truitt, K. C. Schwab, L. Sekaric, J. M. Parpia, H. G. Craighead, and J. E. Butler, Appl. Phys. Lett. **84**, 972 (2004).
[2]A. N. Cleland and M. L. Roukes, Appl. Phys. Lett. **69**, 2653 (1996).
[3]B. Ohler, Rev. Sci. Instrum. **78**, 063701 (2007).
[4]K. L. Ekinci and M. L. Roukes, Rev. Sci. Instrum. **76**, 061101 (2005).
[5]K. Y. Yasumura, T. D. Stowe, E. M. Chow, T. Pfafman, T. W. Kenny, B. C. Stipe, and D. Rugar, J. Microelectromech. Syst. **9**, 117 (2000).
[6]S. Evoy, A. Olkhovets, L. Sekaric, J. M. Parpia, H. G. Craighead, and D. W. Carr, Appl. Phys. Lett. **77**, 2397 (2000).
[7]K. L. Ekinci, Y. T. Yang, and M. L. Roukes, J. Appl. Phys. **95**, 2682 (2004).
[8]K. L. Ekinci, X. M. H. Huang, and M. L. Roukes, Appl. Phys. Lett. **84**, 4469 (2004).
[9]V. Sazonova, Y. Yaish, H. Ustunel, D. Roundy, T. A. Arias, and P. L. McEuen, Nature **431**, 284 (2004).
[10]C. W. Pao and D. J. Srolovitz, Phys. Rev. Lett. **96**, 186103 (2006).
[11]C. Friesen and C. V. Thompson, Phys. Rev. Lett. **89**, 126103 (2002).
[12]I. Harald, Surf. Sci. Rep. **29**, 195 (1997).
[13]M. L. Roukes, Sci. Am. **285**, 48 (2011).
[14]P. Mohanty, D. A. Harrington, K. L. Ekinci, Y. T. Yang, M. J. Murphy, and M. L. Roukes, Phys. Rev. B **66**, 085416 (2002).
[15]D. W. Carr, S. Evoy, L. Sekaric, H. G. Craighead, and J. M. Parpia, Appl. Phys. Lett. **75**, 920 (1999); L. Sekaric, J. M. Parpia, H. G. Craighead, T. Feygelson, B. H. Houston, and J. E. Butler, *ibid.* **81**, 4455 (2002).
[16]X. M. H. Huang, Ph.D. thesis, California Institute of Technology, 2004, p. 36.
[17]G. Palasantzas, Appl. Phys. Lett. **90**, 041914 (2007).
[18]G. Palasantzas, Appl. Phys. Lett. **91**, 021901 (2007); J. Appl. Phys. **102**, 076111 (2007); *ibid.* **101**, 076103 (2007).
[19]K. L. Ekinci, D. M. Karabacak, and V. Yakhot, Phys. Rev. Lett. **101**, 264501 (2008).
[20]O. Ergincan, G. Palasantzas, and B. J. Kooi, Phys. Rev. B **85**, 205420 (2012).
[21]H. Hosaka, K. Itao, and S. Kuroda, Sens. Actuators, A **49**, 87–95 (1995).
[22]S. Bianco, M. Cocuzza, S. Ferrero, E. Giuri, G. Piacenza, C. F. Pirri, A. Ricci, L. Scaltrito, D. Bich, A. Merialdo, P. Schina, and R. Correale, J. Vac. Sci. Technol. B **24**, 1803 (2006).
[23]B. N. J. Persson, J. Chem. Phys. **115**, 3840 (2001).
[24]G. Palasantzas, Phys. Rev. B **48**, 14472 (1993).